Investigation of the pressure and flow dynamics during aspiration thrombectomy: A mathematical modelling study

Riccardo Marconi[1], Ying Yang[1] and Shailesh Naire[2] *
[1] School of Pharmacy and Bioengineering, Keele University, Keele, Staffordshire, ST5 5BG, UK
[2]School of Computing and Mathematics, Keele University, Keele, Staffordshire, ST5 5BG, UK

*email: s.naire@keele.ac.uk

Abstract. Aspiration thrombectomy is a life-saving interventional procedure to remove a blood clot from the brain of stroke patients. The pressure and blood flow dynamics during this procedure are crucial in determining the clinical outcomes. A mathematical model based on Hagen-Poiseuille law of fluid flow in a tube is adapted to simulate the pressure and fluid flow characteristics in an *in vitro* model of an occluded and unoccluded cerebrovascular network that mimics a poor (unilateral) and good (symmetrical) collateral flow within the Circle of Willis. The results show that in the absence of an occlusion, the pressure and pressure drop are higher in the symmetrical network compared to that in the unilateral network. This is due to the additional limb in the symmetrical network that must be supplied, which is absent in the unilateral network. In the presence of an occlusion, the flow reduces in the obstructed vessel, the collateral flow, overall pressure and pressure drop increases in both systems, but is higher for the symmetrical network. The results compare qualitatively with those observed in *in vitro* studies and with clinical observations. The theoretical framework lays the foundation for more advanced models for the pressure and blood flow dynamics towards clinical applicability.

1. Introduction

A stroke is a serious life-threatening medical condition. It is the 2nd leading cause of mortality worldwide [1]. Approximately 85% of strokes are of ischemic nature caused by a thrombus occluding one or more arteries in the cerebral vasculature, leading to the reduction of cerebral blood flow (CBF). When CBF is interrupted for 30 seconds, there are complex modifications in brain metabolism [2]. However, in ischemic stroke, CBF is often disrupted for a longer period and the extent/evolution of the ischemic damage, predominately through damage of surrounding tissue due to cell death, is determined by the time it takes to re-establish circulation [3,4]. It has been reported that 1.9 million neurons, 14 billion synapses and 12 km of myelinated fibres are destroyed within one minute; rapid neuronal death can continue between a period of 6 and 18 hours after a stoke [4,5].

Following an occlusion, tissue immediately surrounding the occluded vessel - the ischemic core - is the area of extensive irreversible ischemia [3], whereas tissue adjacent to the core - the penumbra - is an 'at risk' region, in contrast [6,7]. The impact of hypo-perfusion to these tissues does not affect to the same extent and time than that experienced at the core, and thus can be salvaged if prompt therapeutic intervention is conducted [8]. Consistent with this, evidence with both animal and human studies suggest that intervention and early restoration of CBF following the onset of a stroke is essential for the improved outcome/recovery of the patient and reduced brain injury [9–11].

Currently, intravenous thrombolysis and endovascular treatment via mechanical thrombectomy (MT) remain the two approved therapeutic modalities. MT involves guiding a catheter through the cerebrovascular network to the location of the clot and then using either a stent retriever or aspiration (suction) device to remove it. MT demonstrates significantly higher recanalization (reopening) rates, however, clinical outcomes using suction are often variable [11]. Understanding the pressure and flow dynamics during this procedure are crucial in determining the clinical outcomes, and in the control and accuracy of this interventional procedure.

Benchtop experiments mimicking the MT procedure in a glass model system of the cerebrovascular network have been pioneered by Tennuci *et al.* [12] and Lally *et al.* [13] (figure 1 A). More recently, Dinama [14] adapted the *in vitro* model to study collateral flow in the Circle of Willis network represented by a unilateral network (characterising poor collateral flow; figure 1 B) and symmetrical network (characterising good collateral flow; figure 1 B) with an occlusion in the Middle Cerebral Artery (MCA).

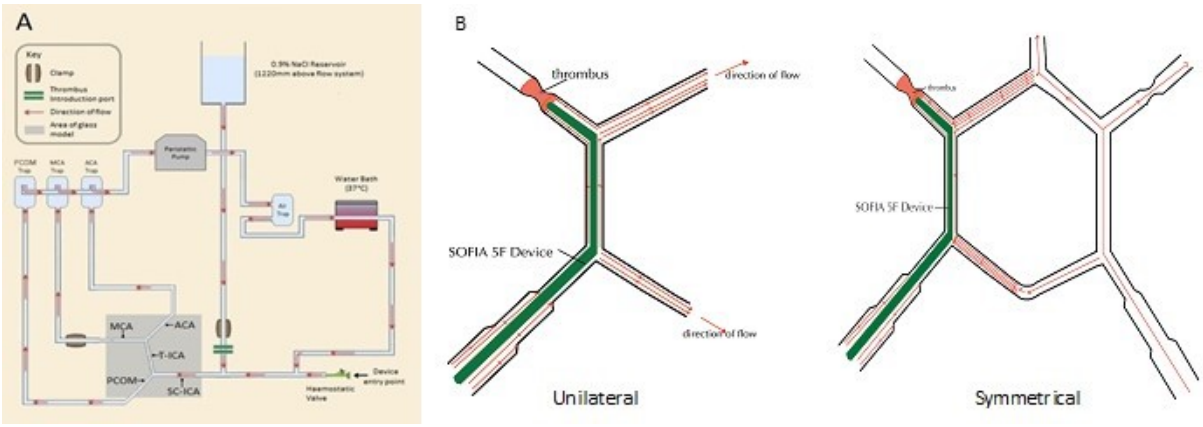

Figure 1. A. Benchtop pulsatile flow and cerebrovascular network model system by Lally *et al.* [13]. The red arrows indicate the direction of the flow. **B.** Unilateral and symmetrical model of the Circle of Willis with occlusion in the MCA adapted by Dinama [14] to replace the section highlighted in grey in the Lally *et al.* model. Figures courtesy Lally *et al.* [13] and Dinama [14].

Pressure sensors were connected to the network to record the changes in pressure as the clot in the MCA was removed using a catheter tube. Dinama [14] showed that a universal pattern of a pressure 'dip' can be observed in the neighbouring branches of the MCA following clot removal (figure 2 A shows the time variations in pressure in the unilateral network - pressure in the MCA is monitored by sensor 2). The dip in pressure in the branching vessels maybe due to the decongestion of the system [14].

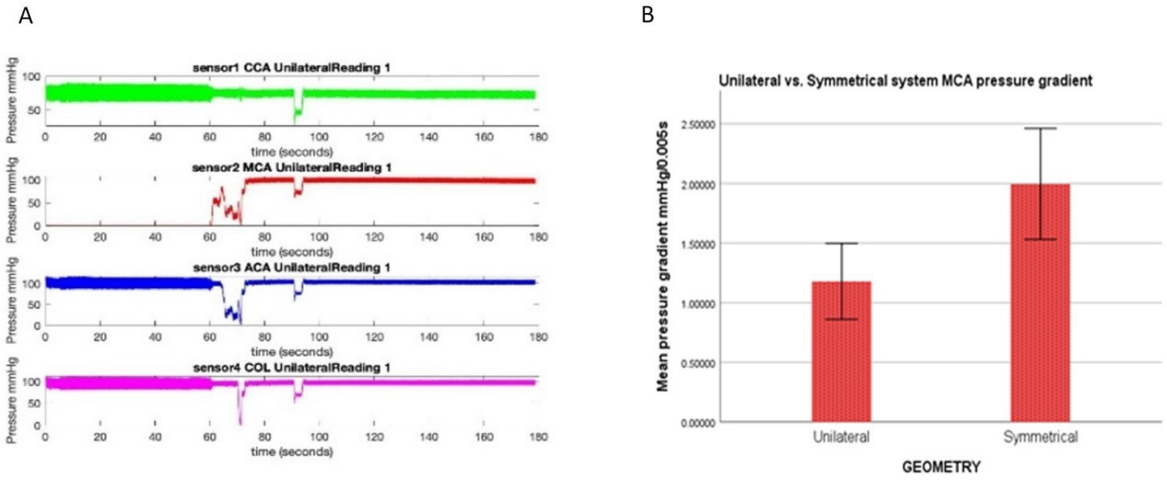

Figure 2. A. Pressure variations during aspiration thrombectomy in the unilateral network. Sensor 2 monitors the pressure in the occluded MCA. **B.** Comparison between the mean pressure gradient (rate of change in pressure) in the unilateral (poor collateral flow) and symmetrical system (good collateral flow). Figures courtesy Dinama [14].

Dinama [14] also reported that the mean pressure gradient (referred to by Dinama as the rate of change in pressure) during clot removal in the symmetrical system was higher than that of the unilateral (figure 2 B). Unfortunately, it is quite expensive and time consuming to run and visualise *in vitro* models; they are also not easily accessible to clinicians.

The main aim of this study is to develop a mathematical model corresponding to the *in vitro* experiments by Dinama [14] in order to understand the pressure and flow variations within the occluded and unoccluded vessels prior to and following clot removal and reperfusion.

2. Methods

A mathematical model of blood flow in a network is developed representing the *in vitro* pulsatile flow system and cerebrovascular network model shown in figure 1 A. This is based on the 0-dimensional modelling approach [15] which focuses on temporal changes in pressure and flowrate in the circulation network, rather than any spatial variations.

2.1 The mathematical model

The mathematical model is based on the Hagen-Poiseuille law of fluid flow in a tube. This relates the flowrate (Q) to the pressure drop along the tube (ΔP) by:

$$Q=C\Delta P,\ C=\pi r^4/8\mu L. \qquad (1)$$

In equation *(1)*, C is the tube compliance (inverse of hydraulic resistance), r and L are the tube radius and length, respectively, and μ is the fluid viscosity. This law is based on the assumptions that the flow is fully developed and quasi-steady in time, and laminar. The typical Reynolds number for the *in vitro* pulsatile system is of the order of a hundred, so as a first approximation we assume the flow is viscous dominated and fluid inertia is neglected, and the flow is driven by the pressure drop across the circulation network.

We adapt the Hagen-Poiseuille law to flow within a network of rigid tubes by applying it to each tube in the network, and using conservation of volumetric flowrate and continuity of pressure at each junction node in the network. An occlusion in a tube is modelled by making its compliance C very small. The removal of the occlusion from a tube and its subsequent reopening is modelled by making the compliance of the tube time dependent, namely,

$$C(t)= (C_{REF}- C_{min})\, H(t-t_0) + C_{min}, \qquad (2)$$

where C_{REF} and C_{min} are a reference and minimum compliance of the tube representing an unoccluded and occluded tube, respectively, t_0 is the time of reopening, and $H(t-t_0)$ represents the Heaviside function which is zero if $t<t_0$, and one otherwise. A time sequence of the removal of the occlusion and subsequent reopening of each vessel that the occlusion passes through in the network is modelled using a combination of Heaviside functions. The temporal dynamics in the pressure and flowrate is investigated in response to the changes in compliance and the boundary conditions (described in section 2.3 below).

2.2 Circuit diagrams

Figure 3 shows a schematic of the unilateral (A) and symmetrical (B) system mimicking collateral flow in the Circle of Willis *in vitro* model studied in Dinama [14]. The arrows show the hypothesised flow direction through the network.

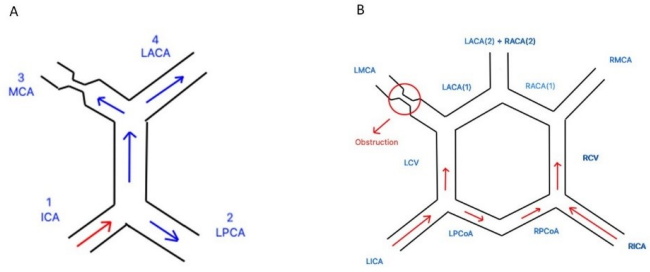

Figure 3. Sketch of **A.** unilateral and **B.** symmetrical system based on Dinama [14]. Arrows indicate the hypothesised direction of the flow through the network.

Figure 4 shows the circuit diagrams for the unilateral (A) and symmetrical (B) systems mimicking the pulsatile flow system in Dinama [14].

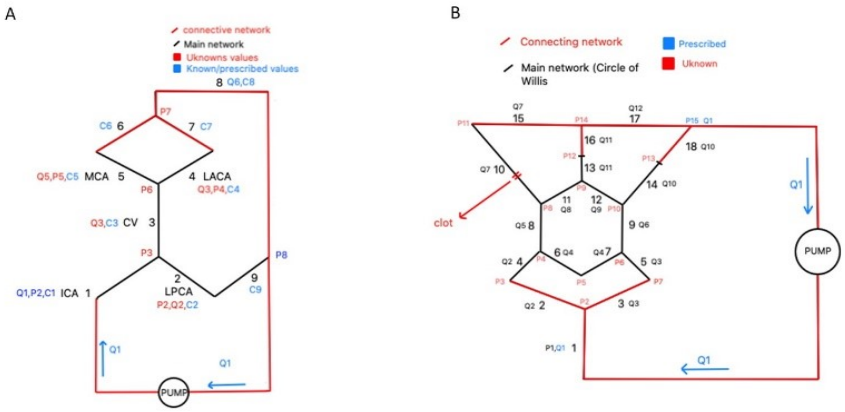

Figure 4. Circuit diagram mimicking the pulsatile flow system in Dinama [14] for **A.** unilateral and **B.** symmetrical network. The numbering of the pressures and flowrates in each tube in the network are shown for future reference.

2.3 Boundary conditions and parameter values

At the system inlet (ICA), the flowrate Q_1=247mL/min is prescribed, based on a typical adult ICA flowrate [16]. The outlet blood pressure (*p8 and p18* for the unilateral and symmetrical network, respectively) is 80 mmHg. Parameter values for the blood viscosity and the mean length and diameter of the vessels in the Circle of Willis is obtained from the literature, and used to calculate the compliance parameter values for each vessel in the Circle of Willis. Approximate values for the compliance of the vessels outside the Circle of Willis are chosen so as to obtain both realistic and comparable behaviour between the two representations.

2.4 Model equations

We obtain a system of equations for the pressure P and flowrate Q for each vessel in the network using *Eq. (1)*, and conservation of flow and continuity of pressure at each junction node. They are parametrised by the compliance for each vessel. These equations are solved simultaneously in Wolfram Mathematica [17] for a prescribed inlet flowrate, outlet pressure, and prescribed function for the compliance in the case of an occlusion or removal of occlusion from the system (see section 2,1).

3. Results and Discussions

3.1 Flowrate and pressure with and without MCA occlusion in unilateral and symmetrical networks

The baseline compliance parameter of the MCA (vessel number 5 for the unilateral and 10 for symmetrical network in Figure 4) is $C_{MCA,\,REF}$=1.5 mm^4 kg s^{-1}, and the occlusion in the MCA is assumed to reduce the compliance by 4/5^{ths} of the baseline value, so $C_{MCA,\,MIN}$= $C_{MCA,\,REF}$/5=0.3. In the absence of the MCA occlusion, the flowrate Q_5, indicating the flow in the MCA for the unilateral network, is calculated to be 0.537mL/s while the flowrate in the corresponding collateral vessel Q_4 (denoted by LACA) is 0.258 mL/s. When the MCA is occluded in the unilateral network, Q_5 is reduced to 0.2039mL/s (-62%) while the flow in the collateral vessel LACA increases to Q_4=0.293 mL/s (+13%). The pressure at the inlet P_1, driving the fluid through the system, increases from 81.889 to 81.961mmHg (+0.08%) and the pressure in the occluded vessel P_5 reduces from 80.366 to 80.139 mmHg when the MCA is occluded (-0.29%).

For the symmetrical network, in the absence of the MCA occlusion, the flowrate in the MCA is calculated to be Q_7=1.149 mL/s, while the flowrate of the collateral vessel LACA (1) (denoted by vessel

11) is Q_8=0.298 mL/s. The corresponding flowrate in the MCA and LACA (1), when the occlusion is introduced is Q_7=0.617 mL/s (-46%) and Q_8=0.478 mL/s (+60%), respectively. The pressure at the MCA P_{11} reduces from 82.962 mmHg in the absence of the occlusion, to 82.200 mmHg (-0.9%), while the inlet pressure P_1 increases from 84.389 mmHg to 84.855 mmHg (+0.55%).

The reduction of pressure and flow rates within the MCA for both the unilateral and symmetrical networks are consistent with measurements of CBF and pressure in rat studies by Overgaard *et al.* [18].

3.2 Comparison of pressure drop between unilateral and symmetric networks

The pressure drop in the MCA in the symmetrical network P_8-P_{11} is 2.084 mmHg and 0.774 mmHg in the presence and absence of the occlusion, respectively. While in the unilateral system, the pressure drop across the MCA P_6-P_5 is 0.689 mmHg and 0.363 mmHg in the presence and absence of the occlusion, respectively, which is lower compared to the symmetrical case. The mean pressure gradient in the symmetrical network is 1.429 mmHg and 2.581 mmHg in the presence and absence of the occlusion, respectively, while for the unilateral network it is 0.253 mmHg and 0.526 mmHg, respectively.

The increased pressure and pressure drop in the symmetrical network is due to the additional limb that must be supplied which is absent in the unilateral network. The branching network surrounding the occluded vessel has to bear the flow burden due to this. This observation is supported by Liu *et al*., [19] in the cardiovascular system where the external carotid artery a possible limb of collateral flow when the internal carotid artery is occluded.

Within the symmetrical system, a higher pressure drop is reported compared to the unilateral system consistent with the *in vitro* investigation by Dinama [14]. In the presence of a good collateral network, the CBF diverges more effectively throughout the network surrounding the occlusion, hence, resulting in a reduction in the pressure drop at the occluded portion of the system. Clinical studies have indicated that patients who had a good degree of collateral flow reported a positive neurological outcome for both thrombolysis and MT [20,21].

3.3 Time-dependent flowrate and pressure during removal of occlusion

We have also simulated the time-dependence of the pressure and flowrate in each vessel as the occlusion is removed out of the system by using a combination of Heaviside functions (described in section 2.1). These results are not shown here due to page limit constraints but confirm the static results above and are qualitatively similar to the *in vitro* results of Dinama [14] shown in figure 2 A.

4. Conclusions

The mathematical model captures qualitatively many features of the variations in the blood flow and pressure in an occluded and unoccluded cerebrovascular network reported in *in vitro* and *in vivo* studies.

While the model reproduces many features of the global dynamics of the cerebrovascular circulatory system, it disregards key components, such as the effect of suction on the flow and pressure dynamics [13], the role of fluid inertia, spatial variations of pressure and flow, and many others. Future studies need to implement advanced models to have a more accurate representation of the flow and pressure dynamics.

References

[1] Gorelick P B 2019 The global burden of stroke: persistent and disabling *Lancet Neurol* **18** 417–8.

[2] Caplan L R 2016 *Caplan's Stroke: A Clinical Approach* (Cambridge University Press).

[3] Sims N R and Muyderman H 2010 Mitochondria, oxidative metabolism and cell death in stroke *Biochim Biophys Acta BBA - Mol. Basis Dis* **1802** 80–91.

[4] Jaffer H, Morris V B, Stewart D, and Labhasetwar V 2011 Advances in stroke therapy *Drug Deliv Transl Res* **1** 409–19.

[5] Saver J L 2006 Time is brain - Quantified *Stroke* **37** 263–6.

[6] Tóth OM, Menyhárt Á, Frank R, Hantosi D, Farkas E, and Bari F 2020 Tissue acidosis associated with ischemic stroke to guide neuroprotective drug delivery *Biology* **9** 460.
[7] Belayev L, Zhao W, Busto R, and Ginsberg M D 1997 Transient middle cerebral artery occlusion by intraluminal suture: I. three-dimensional autoradiographic image-analysis of local cerebral glucose metabolism - blood flow interrelationships during ischemia and early recirculation *J Cereb Blood Flow Metab* **17** 1266–80.
[8] Jordan J D and Powers W J 2012 Cerebral autoregulation and acute ischemic stroke *Am J Hypertens* **25** 946–50.
[9] Tanaka Y, Nakagomi N, Doe N, Nakano-Doi A, Sawano T, Takagi T, Matsuyama T, Yoshimura S, and Nakagomi T 2020 Early reperfusion following ischemic stroke provides beneficial effects, even after lethal ischemia with mature neural cell death *Cells* **9** 1374.
[10] Khatri P, Abruzzo T, Yeatts S D, Nichols C, Broderick J P, and Tomsick T A 2009 Good clinical outcome after ischemic stroke with successful revascularization is time-dependent *Neurology* **73** 1066–72.
[11] Rha J-H and Saver J L 2007 The impact of recanalization on ischemic stroke outcome: a meta-analysis *Stroke* **38** 967–73.
[12] Tennuci C, Pearce G, Wong J, Nayak S, Jones T, Lally F, and Roffe C 2011 Comparison of the effectiveness of three methods of recanalization in a model of the middle cerebral artery: Thrombus aspiration via a 4F catheter, thrombus tspiration via the GP thromboaspiration device, and mechanical thrombectomy using the solitaire thrombectomy device *Stroke Res Treat* **2011** 1–6.
[13] Lally F, Soorani M, Woo T, Nayak S, Jadun C, Yang Y, McCrudden J, Naire S, Grunwald I, and Roffe C 2016 In vitro experiments of cerebral blood flow during aspiration thrombectomy: potential effects on cerebral perfusion pressure and collateral flow *J NeuroInterventional Surg* **8** 969–72.
[14] Dinama E 2019 *Investigation of pressure dynamics during mechanical thrombectomy in a stroke model: effect of device type, size and patient vessel geometry.* unpublished (Keele University).
[15] Shi Y, Lawford P and Hose R 2011 Review of zero-d and 1-d models of blood flow in the cardiovascular system *BioMed Engrg* online, **10** 33.
[16] Skytioti M, Søvik S, and Elstad M 2016 Internal carotid artery blood flow in healthy awake subjects is reduced by simulated hypovolemia and noninvasive mechanical ventilation *Physiol. Rep* **4** e12969.
[17] Wolfram Research, Inc. 2020 Mathematica version 12.2.
[18] Overgaard K, Sereghy T, Boysen G, Pedersen H, Høyer S, and Diemer N H 1992 A Rat model of reproducible cerebral infarction using thrombotic blood clot emboli *J. Cereb Blood Flow Metab* **12** 484–90.
[19] Liu J, Wang Y, Akamatsu Y, Lee C C, Stetler R A, Lawton M T, and Yang G-Y 2014 Vascular remodelling after ischemic stroke: mechanisms and therapeutic potentials *Prog Neurobiol* **115** 138–56.
[20] Kucinski T, Koch C, Eckert B, Becker V, Krömer H, Heesen C, Grzyska U, Freitag H, Röther J, and Zeumer H 2003 Collateral circulation is an independent radiological predictor of outcome after thrombolysis in acute ischaemic stroke *Neuroradiology* **45** 11–8.
[21] Cohen J E and Leker R R 2013 Revascularization-outcome paradox: not only time and collaterals status, but also complete recanalization contribute to good neurological outcome *Int J Stroke* **8** 542–4.